Chemistry & Biology, Vol. 12, 825–833, July, 2005, ©2005 Elsevier Ltd All rights reserved. DOI 10.1016/j.chembiol.2005.05.015

Shift to Pseudomonic Acid B Production in *P. fluorescens* NCIMB10586 by Mutation of Mupirocin Tailoring Genes *mupO*, *mupU*, *mupV*, and *macpE*

Sian M. Cooper,[1,3] Wanpen Laosripaiboon,[2] Ayesha S. Rahman,[1] Joanne Hothersall,[1] A. Kassem El-Sayed,[1,4] Christopher Winfield,[2] John Crosby,[2] Russell J. Cox,[2] Thomas J. Simpson,[2] and Christopher M. Thomas[1,*]

[1]School of Biosciences
University of Birmingham
Edgbaston
Birmingham B15 2TT
United Kingdom

[2]School of Chemistry
University of Bristol
Cantock's Close
Bristol BS8 1TS
United Kingdom

Summary

Mupirocin, a polyketide-derived antibiotic from *Pseudomonas fluorescens* NCIMB10586, is a mixture of pseudomonic acids (PA) that target isoleucyl-tRNA synthase. The *mup* gene cluster encodes both type I polyketide synthases and monofunctional enzymes that should play a role during the conversion of the product of the polyketide synthase into the active antibiotic (tailoring). By in-frame deletion analysis of selected tailoring open-reading frames we show that *mupQ*, *mupS*, *mupT*, and *mupW* are essential for mupirocin production, whereas *mupO*, *mupU*, *mupV*, and *macpE* are essential for production of PA-A but not PA-B. Therefore, PA-B is not simply produced by hydroxylation of PA-A but is either a precursor of PA-A or a shunt product. In the *mupW* mutant, a new metabolite lacking the tetrahydropyran ring is produced, implicating *mupW* in oxidation of the 16-methyl group.

Introduction

A wide variety of compounds of pharmaceutical value are derived at least in part via polyketide biosynthetic pathways [1]. One of the most interesting discoveries in recent years concerns the type I modular polyketide synthases (PKS) that consist of megaproteins, in which every addition to the growing polyketide chain is catalyzed by a distinct module, each of which contains a ketosynthase (KS) domain [2]. In such multifunctional polypeptides, the chemical structure elaborated by subsequent selective keto reduction, dehydration, and enoyl reduction after the condensative addition of an extender unit can be predicted from the enzymatic activities present in each module, via sequence alignments, as exemplified first by the erythromycin-biosynthetic cluster [3]. Once the polyketide-synthase-derived core is produced, it is often further modified by a series of tailoring steps, which may be changes to the backbone or addition of moieties such as sugars. Formation of hybrid PKS systems to produce novel products has been extensively reviewed [4–7]. There have been fewer examples of manipulation of the tailoring genes, but the recent production of prerapamycin provides a powerful example [8]. Rational use of this approach depends on understanding the role of each enzyme in the biosynthetic cluster.

Mupirocin, a polyketide-derived antibiotic produced by *Pseudomonas fluorescens* NCIMB10586, inhibits isoleucyl-tRNA synthase and is used to control infections by methicillin-resistant *Staphylococcus aureus*, MRSA [9]. The mupirocin structure consists of two elements, monic acid (MA) and 9-hydroxy-nonanoic acid (**1**, 9-HN), joined by an ester linkage [10–12] (Figure 1). Analysis of the fate of isotopically labeled precursors [13, 14] gave rise to a plausible biosynthetic pathway for the primary carbon chain of monic acid that fits well with the biosynthetic enzyme activities predicted from the DNA sequence of the cluster (Figure 2) [15]. It is less obvious how 9-HN is made and a number of possibilities have been described previously [15]. As with many other natural products, mupirocin is a mixture of more than one compound—termed pseudomonic acids, of which PA-A to PA-D (compounds **1** to **4**) are the most common (Figure 1). A second group of related secondary metabolites isolated from the marine bacterium, *Alteromonas rava*, the thiomarinols, have very similar structures (compounds **5** to **8**) and may be the product of closely related genes (Figure 3) [16, 17]. Apart from all lacking the 10,11-epoxide, they show structures that suggest similar tailoring steps to those involved in PA-A biosynthesis, and consideration of these may help to interpret available information about mupirocin. The different related compounds observed in both these systems may be intermediates from the pathway or could be shunt products. However, one of the most intriguing questions arising from analysis of the *mup* cluster is why there are so many tailoring enzymes because there would appear to be many more than are necessary for the number of additional modification steps involved in the biosynthetic pathway.

The work described here is part of a larger study to determine the role that each of the individual protein-coding genes in the tailoring region plays in the biosynthesis of mupirocin. It is already clear that the *mup* cluster does not follow the simple relationship between gene order and biosynthetic order exhibited by the erythromycin and most other modular type I genes [3]. This study focused on the genes closest to the downstream end of the cluster, relative to the major direction of transcription. The region chosen for the subject of this study was defined at the upstream end by *mupM* and *mupN*, which encode obvious functions (mupirocin-resistant isoleucyl tRNA synthase and phospho-

*Correspondence: c.m.thomas@bham.ac.uk
[3]Present address: Biotica Technology, Ltd., Chesterford Research Park, Little Chesterford, Nr Saffron Walden, Essex CB10 1XL, United Kingdom.
[4]Present address: Botany Department, Faculty of Sciences (Damietta), University of Mansoura, Damietta El-Gededa, PO Box 35417, Egypt.

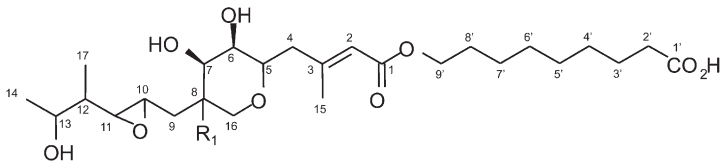

Pseudomonic Acid	A **1**	B **2**	C **3**	D **4**
R_1	H	OH	H	H
C10-C11	Epoxide	Epoxide	Alkene	Epoxide
C4'-C5'	Alkane	Alkane	Alkane	Alkene

Figure 1. The Structures of the Major Pseudomonic Acids

Pseudomonic acid A (PA-A) (compound 1) forms 90% ; PA-B (compound 2) forms 8%; PA-C (compound 3) forms <2% ; and PA-D (compound 4) forms <0.2%.

pantetheinyl transferase, respectively), and at the downstream end by the transcriptional terminator after *mupX*. Deletions of *mupR* and *mupS* in this region have previously been reported to result in complete loss of antibiotic production [15–18]. The *mupP* region was not targeted in this study because establishing which orf if any is active will involve considerable work—the most obvious candidate is encoded on the opposite strand to most other genes in the cluster, but it is not clear if it will be expressed. Therefore *mupO*, *mupQ*, *mupT*, *mupU*, *mupV*, *mupW*, and *mupX* were selected for genetic analysis followed by identification of intermedi-

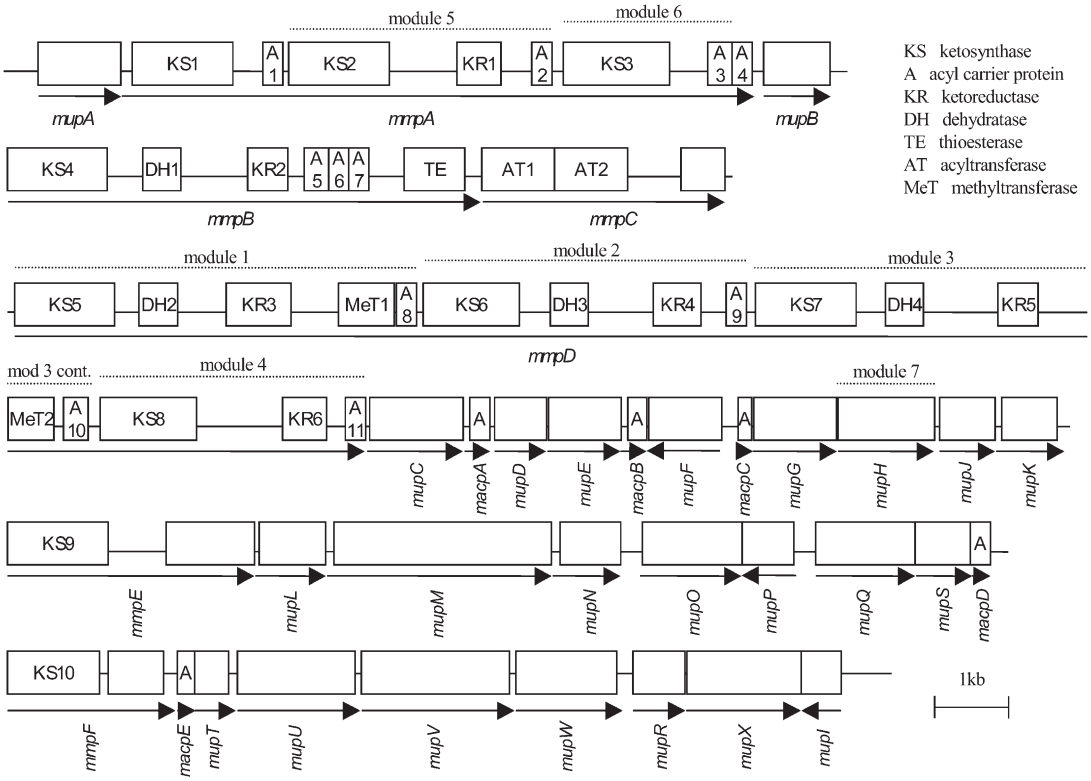

Figure 2. Summary of the Mupirocin Biosynthetic Gene Cluster

Boxes represent functional domains of polypeptides. Arrows below the boxes represent ORFs, indicating also the direction of transcription.

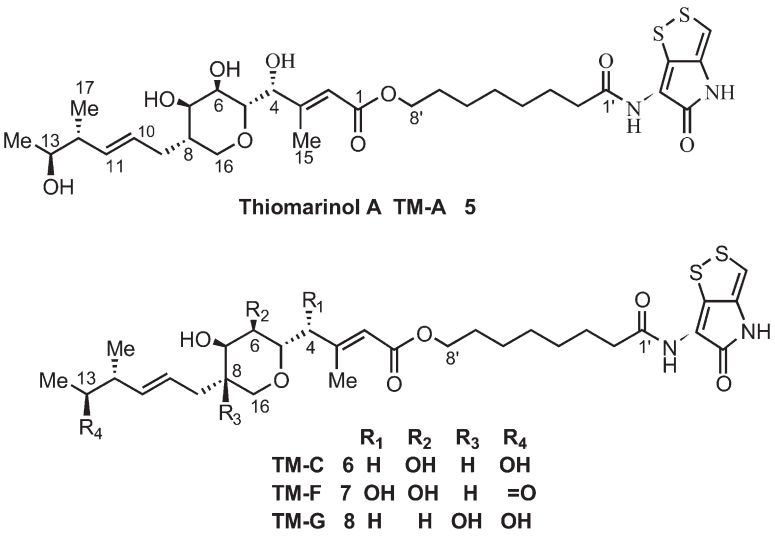

Figure 3. Thiomarinol-Related Compounds

Structure of thiomarinol metabolites or precursors as determined previously [16, 17–36].

ates that might be produced with HPLC, mass spectrometry, and then NMR spectroscopy in selected cases. The results show that the genes encode late biosynthetic steps and suggest that multiple genes may work together to catalyze individual tailoring steps.

Results

All Genes Clustered at the Downstream End of the *mup* Region Are Required for Normal Mupirocin Biosynthesis

In-frame chromosomal deletions were constructed in each of the selected genes—*mupO* encoding a putative cytochrome P450 (339 codons were deleted leaving a polypeptide of 116 aa), *mupQ* encoding a putative acyl-CoA synthase (145 codons were deleted leaving a polypeptide of 307 aa), *mupT* encoding a putative ferredoxin dioxygenase (58 codons were deleted leaving a polypeptide of 59 aa), *mupU* encoding a second putative acyl-CoA synthase (501 codons were deleted leaving a polypeptide of 24 aa), *mupV* encoding a putative oxidoreductase (596 codons were deleted leaving a polypeptide of 67 aa), *mupW* encoding a putative dioxygenase (350 codons were deleted leaving a polypeptide of 114 aa), and *mupX* encoding a putative amidase or hydrolase (415 codons were deleted leaving a polypeptide of 98 aa). As part of a separate study of the acyl carier proteins (to be published fully elsewhere) *macpE* was also inactivated in a similar manner, deleting 71 codons to leave a polypeptide of just 6 aa from the start and 3 aa from the end of the protein. It is included here because of the phenotype it generates as described below. In-frame deletions were made to minimize polar effects so that the resulting phenotype should be the result of specifically knocking out the target gene (or genes) and not because of the decreased expression of downstream, nontarget genes. The specific deletions in the target genes were created between two flanking arms, each at least 500 bp in length as described in Experimental Procedures.

A suicide vector system, pAKE604, was used to insert these deletions into the chromosome as described in Experimental Procedures [15]. Antibiotic production by the mutants was evaluated with the plate bioassay (see Experimental Procedures), which assessed the ability of the experimental strains to produce mupirocin, indicated by the average area in cm^2 of their zone of inhibition relative to the size of wild-type zone. The wild-type strain gave an average area of 10.1 cm^2, and a mutant strain, AKE3 (Δ*mupI*) [18], used as a "nonproducer" control, gave an average halo area of 1.8 cm^2. Each mutant demonstrated reduced antibiotic activity to varying extents (Figure 4) with Δ*mupQ* and Δ*mupT* effectively indistinguishable from Δ*mupI*. The mutant bioassay phenotypes split into two groups. The first group, containing mutants Δ*mupQ*, Δ*mupT,* Δ*mupW*, and Δ*mupX*, showed a smaller but clear halo. The second group, containing Δ*mupO*, Δ*mupU*, and Δ*mupV*, gave a halo with two distinct regions—a central clear zone surrounded by a more diffuse zone. The Δ*macpE* mutant gave a plate assay phenotype indistinguishable from this second group (data not shown).

Although the mutations were designed not to disrupt transcription or translation of the remainder of the target genes, it is possible that the deletions also reduced the expression of downstream genes (a "polar effect") in the *mup* operon, giving a false phenotype. Therefore, it was necessary to determine whether the mutations could be complemented in trans. All genes of interest were cloned separately into an IncQ-based expression vector (pJH10) as described in Experimental Procedures. Plasmid pJH10 contains a *tac* promoter, an *oriT* region, a multiple cloning site, and a tetracycline resistance gene. The results of these complementation studies were evaluated with the plate bioassay (see Experimental Procedures) on agar with and without IPTG. Inhibition zone sizes were compared with the equivalent strains carrying just the expression vector. Antibiotic production was restored in all the mutants by their respective genes cloned in trans, indicating that the deletions did not have secondary effects. The strains Δ*mup*Q, Δ*mup*W, and Δ*mup*X exhibited better complementation (i.e., bigger zones of inhibition) in the ab-

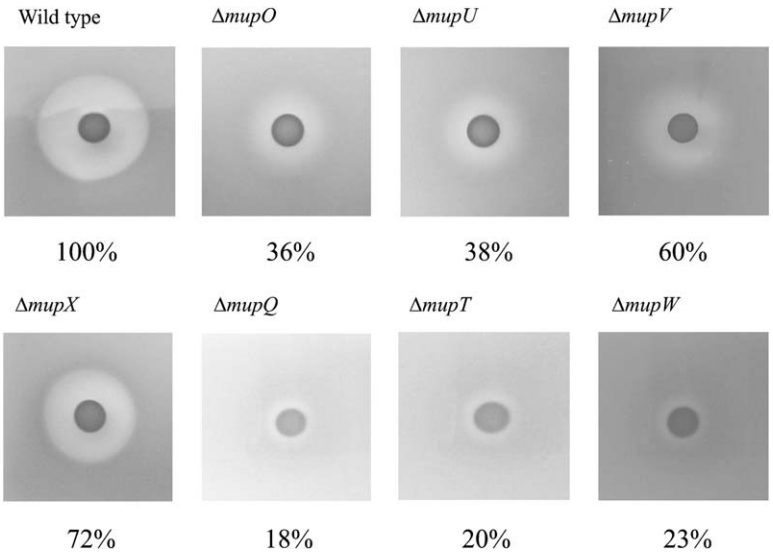

Figure 4. Plate Test Showing Different Phenotypes Observed

With wild-type taken as 100%, the relative size of the zone of inhibition is indicated. The mutants are grouped by phenotype—Δ*mupO*, Δ*mupU*, and Δ*mupV* give a diffuse edge, whereas Δ*mupQ*, Δ*mupT*, Δ*mupW*, and Δ*mupX* give a clear/distinct edge. The data is the mean of three measurements. Standard deviations were of the order of 6% to 10% so that the large differences are significant, whereas the small ones are not.

sence of IPTG, suggesting that low levels of expression (possibly from inefficient translation because it is likely that most if not all the genes are in the same transcriptional unit) (J.H. and C.M.T., unpublished data) are optimal for gene function. However, for Δ*mupO*, Δ*mupT*, and Δ*mupV*, complementation was better in the presence of IPTG, indicating that a higher level of gene expression is optimal. In the absence of IPTG, *macpE* in trans restored mupirocin production to wt levels (100%), whereas in the presence of 0.1 mM and 0.5 mM IPTG, the zones of inhibition were slightly reduced (85%) when compared to wt.

Because sequence alignments suggest that both MupQ and MupU may have acyl-CoA ligase activities, it was possible that they might be able to substitute for each other. Because knocking out each one individually resulted in different but significant defects in antibiotic production, there clearly is not complete functional redundancy between them. Nevertheless, we created a double mutant to check whether this gave a more severe defect compared to either knock out alone. The phenotype of the Δ*mupQU* double mutant in the plate bioassay is indistinguishable from that of the single Δ*mupQ* mutation that gives the more severe of the two mutant phenotypes, suggesting that they do not provide alternative ways of achieving the same step. This was confirmed by overproducing *mupU* in trans to Δ*mupQ* and overproducing *mupQ* in trans to Δ*mupU*, which showed no evidence for any cross complementation between these two genes.

HPLC Analysis of the Products of the WT and Mutant Strains

The HPLC profile of the supernatant from stationary phase cultures of wt NCIMB10586 strain under the conditions described in Experimental Procedures and with detection at 233 nm (Figure 5) revealed one major peak (peak 1) whose retention time was 20.5 min, identified by comparison with standard as PA-A 1 (Figure 1), and another smaller peak with retention time 19.6 min (peak

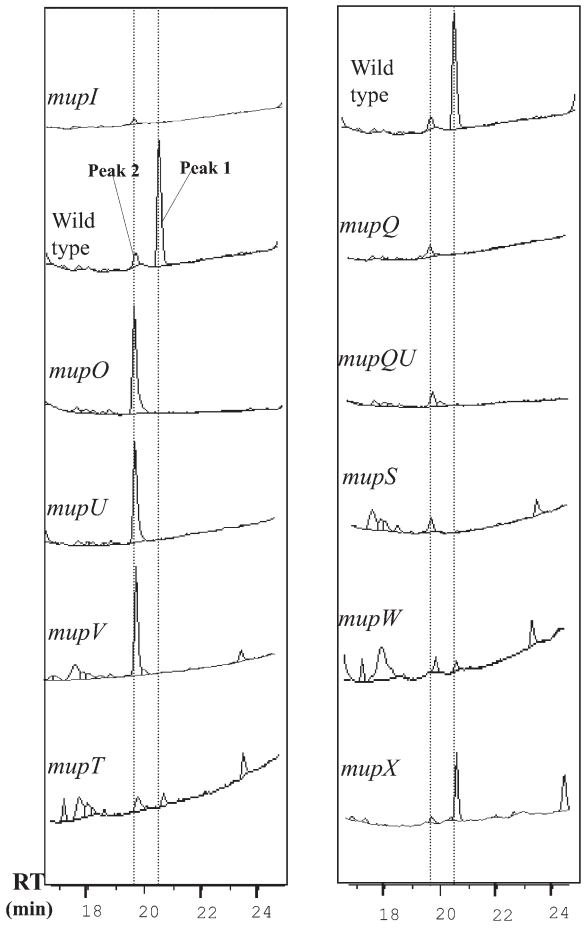

Figure 5. Typical HPLC Traces of the Compounds Detectable at 233 nm Produced by Wild-Type and Mutant Strains

2—PA-B, **2** in Figure 1). A very small peak was also detected at the same position as peak 2 in the profile from the negative control, AKE3(Δ*mupI*), which is defective in expression of the mupirocin biosynthetic pathway [18]. It is likely that some other material also elutes at this position.

Analysis of PA-A peak area by HPLC was carried out for samples taken at different times during growth in mupirocin production medium (MPM) at 22°C after 20-fold dilution of the overnight culture. Mupirocin production had already begun when sampling commenced at 8 hr, but between 8 and 13 hr, a rapid increase in pseudomonic acid production was observed. Maximum antibiotic production (~0.8 μg/ml) was reached at approximately 15 hr, and from this point, levels of PA-A remained relatively constant. The negative control produced only a negligible amount of PA-A throughout the experiment. Therefore, the supernatants of mutant cultures were analyzed at 30 hr. HPLC traces from the broth of the Δ*mupX* strain showed a similar profile to wt but with a smaller area under peak 1 (approximately 85% relative to wt peak 1).

The HPLC traces from the broths of Δ*mupO*, Δ*mupU*, and Δ*mupV* strains all showed the same profile in which peak 1 was absent and peak 2 at 19.55 min was now a similar size to peak 1 in supernatants from wt (70%, 78%, and 122%, respectively, relative to wt peak 1). The Δ*macp*E mutant showed the same profile as these mutants with peak 2 being approximately 60% relative to the size of wt peak 1. Based on area of zones of inhibition, the Δ*macpE* mutant exhibits 64% antibacterial activity when compared to wt. Δ*mupT* and Δ*mupW* broths typically showed similar peak profiles to each other, with only small amounts of detectable material (22% and 17%, respectively, relative to wt). Two peaks were detected that elute slightly later than peaks 1 and 2 (retention time 20.59 min and 19.61 min, respectively). Finally, Δ*mupQ*, Δ*mupQU*, and Δ*mupS* (whose plate bioassay phenotype was reported previously [15]) typically showed less than 10% the level of detectable material relative to wt, and this was concentrated at the position of peak 2. Additional peaks detected at 233 nm with faster or slower elution were sometimes observed for these mutant strains and will eventually be analyzed in detail. However, in this study, we concentrated on the most obvious peaks.

Mass Spectrometric and NMR Analysis of the Products of Selected Mutants

The calculated relative molecular mass (M_r) of PA-A is 500. The mass spectra of the PA-A standard and PA-A purified from the wt broth show very similar profiles. The major peak in both has an M_r of 523, which corresponds to the sodium adduct of PA-A (500 + 23). The spectra of the purified compound from peak 2 produced by Δ*mupO*, Δ*mupU*, Δ*mupV*, and Δ*macpE* showed a major peak with an M_r of 517, corresponding to the hydrogen adduct of PA-A plus an oxygen atom [16]. NMR spectral analysis of this material confirmed the structure as PA-B when compared with values from the literature [12]. The major product of Δ*mup*X (peak 1) was confirmed as PA-A by mass spectrometry and NMR.

Analysis of the product (or products) of Δ*mupT* and Δ*mupW* was more complicated because the total amount of material that accumulated was considerably less than in the mutants described in the previous paragraph. Apart from a small signal corresponding to peak 2, these two mutants showed a new peak at a retention time about 0.5 min slower than PA-A, close to but not identical to peak 1. MS and NMR analysis of the compound isolated from Δ*mupW* showed that this product (PA-W) did not correspond to any of the previously defined PAs but possesses a novel PA structure **10** (Figure 6), which lacks the characteristic tetrahydropyran ring common to all known pseudomonic acids. Detailed structural analysis is described fully elsewhere [19].

Discussion

The genes *mupO*, *mupQ*, *mupS*, *mupT*, *mupU*, *mupV*, *mupW*, and *mupX* were all proposed to be required for tailoring the core structure produced by the type I PKS assembly line. Combined with the data presented previously [15], the results in this paper confirm that indeed all mutations studied do affect mupirocin production. The effect of the deletion in *mupX* is the weakest, simply resulting in an approximately 15% decrease in production of PA-A. It therefore appears that MupX is not essential for any step in the biosynthesis but somehow modifies either the expression of the genes or the efficiency with which enzymes of the pathway proceed. The blast hits and sequence alignments suggest that MupX may have amidase/hydrolase activity. It is possible that MupX represents a relic of an activity that is no longer required but remains because the protein is still a structural component of a multienzyme assembly essential for mupirocin production. In this regard, it may be significant that the thiomarinols have an amide derivative at C-1′ (Figure 2). One can suggest, therefore, that MupX may have had a role in removing an amide derivative.

An important part of our analysis was to demonstrate that each of the mutants could be complemented, showing that the phenotype of the mutation was not because of polar effects. All of the mutants could be complemented, but the level of induction of the *tac* promoter by addition of IPTG that was optimal for complementation varied. It is well known that the *tac* promoter control is leaky, so it is to be expected that there will be a basal level of expression of all the cloned genes in the absence of IPTG. Whether or not addition of IPTG is necessary may reflect differences in the efficiency of expression of the cloned genes or may indicate the levels of proteins normally needed for PA production as well as differences in the consequences of overproduction. Complemented strains in which antibiotic levels are reduced in the presence of IPTG might be expressing proteins that are either toxic to the cell or inhibit the synthesis of mupirocin when expressed at high levels.

Mutation of *mupW* results in the formation of a new metabolite, which we have shown to have the structure **10** (Figure 5) lacking the characteristic tetrahydropyran ring found in the pseudomonic acids and thiomarinols [19]. One possibility is that pseudomonic acid W (**10**) is formed from an acyclic biosynthetic intermediate, e.g.,

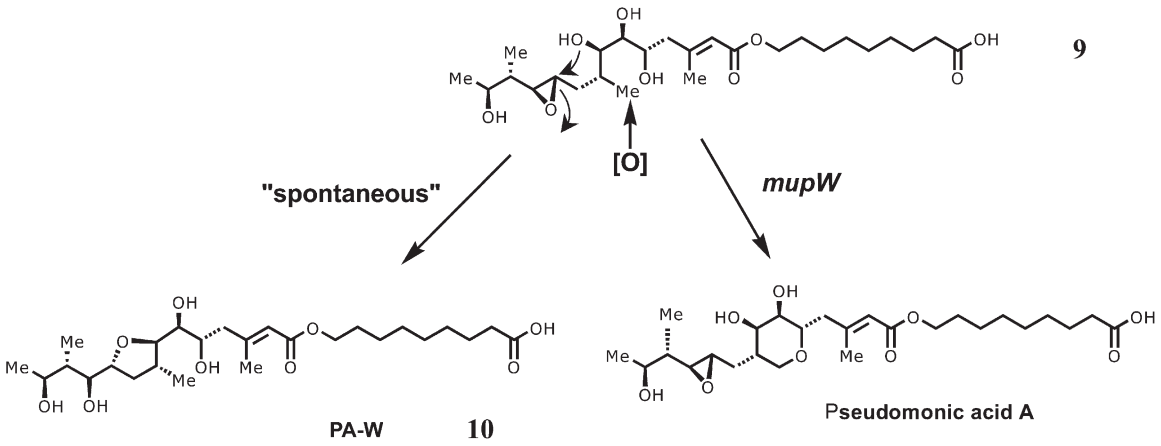

Figure 6. Proposed Action of MupW

Structure of the intermediate PA-W that accumulates in the Δ*mupW* mutant (**10**) [19] and proposed action of MupW on the hypothetical intermediate (**9**) to form the pyran ring. PA-W otherwise spontaneously converts to compound **10**.

9, by opening of a 10,11-epoxide at C-10 by 7-OH (Figure 5). That *mupW* is the gene responsible for 16-hydroxylation would be consistent with its predicted biochemical activity. Mutation of *mupW* blocks hydroxylation, but the other proposed late-stage modifications, 5-hydroxylation, 10,11-epoxidation, and esterification with 9-HN still take place. This implies that it is not essential for MA synthesis to be completed before esterification with 9-HN. MupT may also be involved in this step but has not yet been characterized in more detail.

Of the remaining mutations that generate phenotypes, the most obvious is that exhibited by Δ*mupO*, Δ*mupU*, Δ*mupV*, and Δ*macpE*, which knock out production of PA-A and shift the pathway into producing an equivalent or greater amount of PA-B (80%, 87%, 137%, and 60% relative to wt, respectively). This could suggest that the protein products of these genes are all involved in the same biosynthetic step. MupO is a putative P450 monooxygenase. P450s commonly catalyze reactions involving oxygen transfer, which are typical in post-PKS tailoring. Cytochrome P450 monooxygenases are often found in PKS gene clusters, and there are many cases of their inactivation leading to a structure related to the native antibiotic but lacking a hydroxyl or epoxide group. For example, the disruption of *pimD*, a gene encoding a P450 monoxygenase in the pimaricin gene cluster (*S. natalensis*), results in the formation of 4,5-deepoxypimaricin [20]. In erythromycin biosynthesis, inactivation of *eryF* leads to the accumulation of a derivative lacking the hydroxyl group at C-6 (6-deoxyerythromycin A) [21]. Some atypical reactions performed by P450s have been reported, however, including reductions, dehydrations, dehydrogenations, and isomerizations [22]. Another common feature of P450s is that they function as a part of multicomponent systems, requiring electron transport proteins to shuttle electrons from NAD(P)H [23]. Such a role could be provided by MupV, which is predicted to possess NADPH-dependent reductase activity. MupU is a putative acyl-CoA ligase, the obvious role for which would be activation of an intermediate, prior to the action of MupO and MupV, via an acyl adenylate and independently of CoA. This reaction is similar in rapamycin initiation, occurring at the loading domain of RAPS1 [24]. It can be proposed, therefore, that the biosynthetic step being affected by these mutations is initiated by MupU loading mAcpE with an intermediate, which is then modified by MupO, supported by MupV (Figure 7).

Where in the biosynthetic scheme might this mAcpE-MupU-O-V complex work? According to the predicted mupirocin biosynthetic pathway [15], PA-A would result from epoxidation of PA-C **3** (Figure 1). PA-B would then originate from a simple hydroxylation of PA-A at C8, a commonly observed process in secondary metabolism. However, the accumulation of PA-B at the cost of PA-A production in the mutants reported here indicates that PA-B can not be derived as previously proposed. Indeed, radio-labeling studies conducted by Mantle et al. [25] were also inconsistent with the model that PA-B arises from the oxidation of PA-A. Although it is possible that PA-A may be derived by direct deoxygenation of PA-B, the observed efficient switching from PA-A to PA-B production can perhaps be best explained by diversion of intermediate flux at a key branchpoint (Figure 7). The polyketide precursor **11** predicted from the domain structure of the mupirocin PKS retains an olefinic double bond between carbons 8 and 9. This must be reduced to attain the correct overall oxidation level of PA-A. In a fully processive pathway, this reduction would be predicted to occur via an enoyl reductase (ER) at the tetraketide stage, but the appropriate condensation module 3 lacks an ER domain [15]. The reduction must therefore be carried out by a reductase outside the PKS, and a number of candidate genes can be identified in the mup cluster, e.g., *mupC*, *mupE*, and *mupV*. The timing of this essential reduction step is, however, not apparent. It is relevant to this that the lovastatin nonaketide synthase encoded by *lovA* lacks a functioning ER domain, and this activity is supplied by a separate gene, *lovC*. Expression of *lovA* in the absence of *lovC* results in accumulation of nonreduced

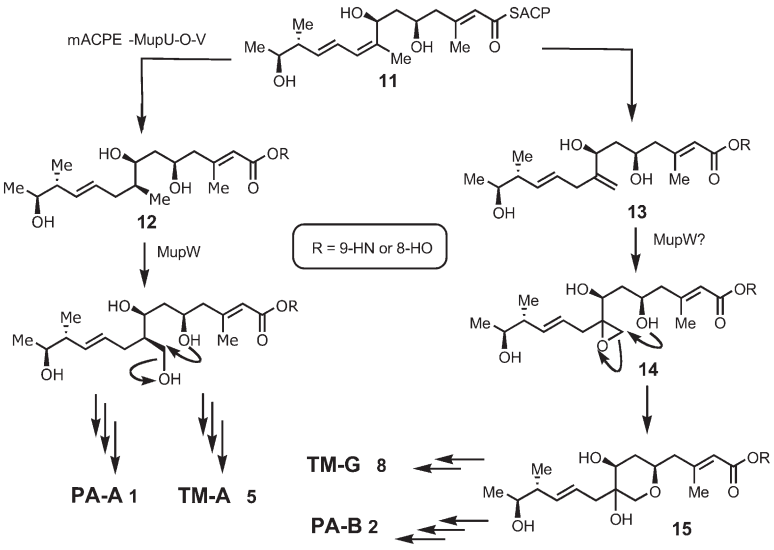

Figure 7. Proposed Scheme to Explain a Branchpoint in the Biosynthetic Pathway

In branch one, the MupO-U-V-mACPE complex catalyzes the reduction of the C8-C9 alkene bond so that the subsequent action of MupW produces a hydroxyl at C16, which then cyclizes to produce the pyran ring. In the absence of the reduction step, isomerization leads to a C8-C16 alkene that produces an epoxide ring with the action of MupW, eventually leading to the PA-B structure as shown.

shunt products [26]. We would thus suggest that the putative MupO-MupU-MupV-mAcpE complex is involved in this key reduction step and so controls the flux of intermediates down this channel. Although there are a number of possibilities, the timing of its intervention would likely be at the end of PKS assembly, or conceivably after addition of 9-HN. Subsequent post-PKS tailoring steps including MupW-initiated cyclisation (Figure 7) would lead to PA-A. Disruption of the full functionality of this complex by any of the reported mutations would lead to PA-B. At this stage, we can only speculate on the mechanism and the genes involved, but an interesting possible mechanism would be isomerization of the 8,9-olefin **11** to give the 8,16-isomer **13**. Subsequent epoxidation to **14**, perhaps also catalyzed by MupW, would allow an alternative mechanism of tetrahydropyran-ring closure, which would form the tetrahydropyran ring and introduce the 8-hydroxyl in one step as shown. The resulting intermediate **15** would require efficient conversion by the remaining tailoring enzymes to produce PA-B in comparable yields to those of PA-A observed in the wt strain. A much-reduced flux of intermediate **11** through this channel would produce the small amounts of PA-B observed in wt and would be consistent with this mechanism. The formation of TM-G **8**, which lacks the extra 4- and 6-hydroxylations, could be circumstantial evidence for the timing of the cyclization. Presumably in this case, intermediate **15**, or TM-G itself, is a less suitable substrate for the tailoring enzymes in *Alteromonas rava* than its counterpart in *Pseudomonas fluorescens*. This hypothesis is testable by isolation and characterization of mACP16 attached to its biosynthetic intermediate, which is a current aim of this laboratory. It is also possible that MupO, MupU, MupV, and mACP16 form a complex that could be isolated by affinity tagging any one of the component proteins. Finally, it is worth noting that the apparent involvement of multiple tailoring genes in a single biosynthetic step may provide a partial answer to why there are so many tailoring genes. Further study of the rest of this region should provide the rest of the explanation.

Significance

The mupirocin biosynthetic cluster has a number of unusual features that distinguish it from many previously studied polyketide biosynthetic pathways. It may thus provide an alternative model system applicable to other natural products such as the thiomarinols. The role of the tailoring genes is the least predictable part of the scheme. This analysis of a selected group of *mup* genes is of great significance in linking genes to biosynthetic function and has prompted us to propose a testable hypothesis for key steps leading to the formation of the central pyran ring in monic acid. This provides an explanation for the synthesis of the two major pseudomonic acids, A and B. Although in this paper we have focused on the mutations that cause the most identifiable shift in biosynthesis, we also report that the *mupW* mutant, which accumulates much less intermediate, is nevertheless informative. A challenge for the future is to determine whether there are minor peaks in other mutants that can also be informative.

Experimental Procedures

Bacterial Strains, Plasmids, and Growth Conditions

The wild-type mupirocin-producing bacterium used in this study was *P. fluorescens* NCIMB 10586 [27]. *Escherichia coli* DH5α was used for plasmid propagation and as the recipient of constructed plasmids in all transformations [28]. The strain *E. coli* S17-1 was used for mobilizing recombinant plasmids into *P. fluorescens* [29]. *Bacillus subtilis* 1604 was used for the determination of mupirocin production by bioassay. Previously described plasmids used were as follows: pGEM-T Easy (Promega); pAKE604 [18]; and pAKE800, pAKE5.8X, pAKE5.8H, and pJH10 [15]. All bacterial strains were routinely grown in LB medium or on L-agar plates [30], except for mupirocin-production-medium (MPM) [27] used when antibiotic biosynthesis was specifically being studied. *P. fluorescens* strains were grown in two stages. For seed cultures, a single colony was used to inoculate 25 ml of primary medium in a 250 ml conical flask and incubated at 25°C, 200 rpm for 24 hr. For mupirocin-production-culture stage, an aliquot of the seed culture was diluted 20-fold into MPM and incubated at 22°C, with shaking at 200 rpm for 45–65 hr. Antibiotics were added to medium as required: penicillin

(Pn) (150 μg/ml in liquid and 300 μg/ml in solid medium), ampicillin (Ap) (50 μg/ml); kanamycin (Km) (50 μg/ml); tetracycline (Tc) (25μg/ml); and mupirocin (Mup) (500 μg/ml).

DNA Isolation and Manipulation

Plasmid DNA was isolated by the alkaline/SDS lysis method [31]. For higher quality plasmid DNA extraction, the Wizard plus SV miniprep purification system manufactured by Promega was used in accordance with the manufacturer's guidelines. A yeast DNA miniprep kit manufactured by Nucleon Tepnel Life Sciences was used to isolate high quality chromosomal DNA. Restriction enzymes were purchased from Gibco BRL, MBI-Fermentas, and New England Biolabs (NEB) and used according to the manufacturer's guidelines. Digested DNA was analyzed by agarose gel electrophoresis in 1× TAE by standard procedures [32]. DNA fragments were purified with the "Geneclean kit" from Bio101. T4 DNA ligase purchased from Gibco BRL was used for ligations and was incubated at 4°C overnight. The ligation reaction was then transformed into *E. coli* DH5α.

PCR reactions were performed as described by Mullis et al. [33]. Template DNA was generated by the standard boiled colony method. Primers were designed to flank the region of interest with extra restriction sites for cloning if needed. Primers were synthesized by Alta Bioscience, University of Birmingham. Table S1, available with this article online, lists all primers designed and used in this study. The DNA polymerases used were Expand High Fidelity system, manufactured by Boehringer Mannheim, for gene cloning and Taq polymerase for confirmation of chromosomal genotype. Glycerol was added to the diagnostic PCR reactions to a final concentration of 5%. PCR product purification was achieved with a HIGH pure purification kit manufactured by Roche. Standard PCR conditions were as follows: denaturation at 94°C for 4 min; 10 cycles of denaturation at 94°C for 30 s, annealing at 59°C for 30 s, annealing at 57°C for 15 s, extension at 72°C for 1.2 min; 20 cycles of denaturation at 94°C for 30 s, annealing at 59°C for 30 s, annealing at 57°C for 15 s, and extension at 72°C for 1.2 min with an increment of 5 s every cycle; final extension at 72°C for 7 min.

Automated DNA Sequencing

DNA sequencing was carried out with Big dye terminating kit manufactured by PE-ABI and was based on the chain termination method [34]. The sequencing PCR-cycling program involved 25 cycles of denaturation at 96°C for 30 s, annealing at 50°C for 15 s and extension at 60°C for 4 min. The ramping time was set to 1°/s. The sequence reactions were run on an ABI 3700 DNA sequencer (Functional Genomics Laboratory, University of Birmingham).

DNA Transfer

Standard methods were used to make *E. coli* strains competent for transformation [35]. Cells were stored at −80°C in 100 mM calcium chloride and 20% glycerol. For mobilization into *P. fluorescens*, the donor strain (*E. coli* S17-1, with appropriate plasmids) was mixed with recipient bacteria on L-agar, incubated at 30°C for 24–30 hr and then spread on solid media containing mupirocin or ampicillin (to kill the donor) and appropriate antibiotic to select for the mobilized plasmid. The transconjugant colonies always grew slowly, requiring incubation at 30°C for up to 72 hr.

Suicide Mutagenesis for Isolation of Chromosomal Mutations

Specific mutations were introduced into the chromosome as previously described [15]. Construction of in-frame deletions was carried out as illustrated with respect to *mupQ* and *mupO*. For *mupQ*, a 1446 bp fragment was amplified by PCR with primers pmupQ-F and pmupQ-R, designed to give flanking *Eco*RI and *Xba*I sites, and cloned into pGEMT-Easy. After cloning, the internal 435 bp *Bst*EII fragment was deleted by standard procedures, leaving the two halves of the orf in frame and flanking arms of 512 bp and 492 bp. The deletion fragment was then cloned into pAKE604. The suicide vector was designated pSCΔQ. For *mupO*, two PCR fragments were amplified, yielding a 601 bp *Eco*RI-*Bam*HI product (primers pmupO1-F and -R) and a 467 bp *Bam*HI-*Xba*I product (primers pmupO2-F and -R) effectively making a deletion of 1197 bp in *mupO* when these were ligated together in pAKE604. The suicide vector was designated pSCΔO. The mutants Δ*mupT*, Δ*mupV*, Δ*mupW*, and Δ*mupX* were also constructed with the same cloning and integration strategy used to generate 10586Δ*mupO* but with primers as listed in Table S1, with the nomenclature as for mup*O*.

Construction of Expression Plasmids and Complementation of Deletion Mutants

The ORFs for each of the genes studied were amplified with the primers listed in Table S1. These primers placed an *Eco*RI site immediately upstream of the start codon and a *Sac*I site immediately downstream of the stop codon. After initial cloning into pGEMT-easy vector, the amplified DNA was checked by sequencing. The *Eco*RI-*Sac*I fragment was then ligated between the *Eco*RI and *Sac*I sites of the Tc^R vector pJH10 [15], placing it downstream of the inducible *tac* promoter. Each recombinant plasmid was designated pSCC followed by the letter corresponding to the gene involved. The expression plasmids were introduced into their corresponding mutant host by biparental mating followed by appropriate selection. As a control the vector, pJH10, with no inserted *mup* gene, was always introduced in parallel.

Determination of Mupirocin Activity and Related Compounds

The plate test for antibacterial activity was performed as described previously [15]. For HPLC quantitative determination of the concentrations of pseudomonic acid and its intermediates from liquid cultures, a calibration curve based on purified mupirocin standard was used. Where a standard did not exist, purified intermediates were dried and weighed.

Purification and Structural Analysis of PA Derivatives

Bacterial liquid cultures were grown in MPM to stationary phase, bacteria removed by centrifugation before acidification to pH 4.5, and then solvent was extracted to exhaustion (three times) with ethyl acetate. After evaporation of the ethyl acetate, the residues were redissolved in methanol and then separated by HPLC in a standard water/acetonitrile gradient (5%–70% acetonitrile over 30 min). HPLC was performed on a Gilson 712 system with UV detector and a reverse phase C18 Supelco Discovery Column (15 cm × 4.6 mm). Alternatively 1 ml samples of 5-fold diluted crude extracts were repeatedly injected and separated with an isocratic gradient (32% acetonitrile, 68% water acidified with 0.01% formic acid), and the appropriate fraction was pooled, dried down and weighed, and used for MS (Kratos Profile Mass Spectrometer, School of Chemical Sciences, University of Birmingham) and NMR (JEOLΔ300, School of Chemistry, University of Bristol).

Supplemental Data

Supplemental Data include one table and can be found with this article online at http://www.chembiol.com/cgi/content/full/12/7/825/DC1/.

Acknowledgments

S.M.C. was supported by the School of Biosciences, University of Birmingham. W.L. was supported by a scholarship from the University of Bristol. A.S.R. was supported by a scholarship from the Darwin Trust of Edinburgh. J.H. was supported by Biotechnology and Biological Sciences Research Council grants P15257 and 07071, which also covered the cost of consumables. C.W. was supported by Biotechnology and Biological Sciences Research Council grant 7/B11480. DNA sequencing was performed in the University of Birmingham Functional Genomics Laboratory, funded by BBSRC grant 6/JIF13209. DNA sequence analysis software was provided by Birmingham Medical Research Council Bioinformatics Project (MRC G.4600017 grant for Bioinformatics Infrastructure). The mupirocin used as standard was a gift from GlaxoSmithKline.

Received: September 22, 2004
Revised: April 11, 2005
Accepted: May 16, 2005
Published: July 22, 2005

References

1. O'Hagan, D. (1995). Biosynthesis of fatty-acid and polyketide metabolites. Nat. Prod. Rep. *12*, 1–32.
2. Staunton, J., and Weissman, K.J. (2001). Polyketide biosynthesis: a millennium review. Nat. Prod. Rep. *18*, 380–416.
3. Donadio, S., Staver, M.J., Mcalpine, J.B., Swanson, S.J., and Katz, L. (1991). Modular organization of genes required for complex polyketide biosynthesis. Science *252*, 675–679.
4. Khosla, C. (1997). Harnessing the biosynthetic potential of modular polyketide synthases. Chem. Rev. *97*, 2577–2590.
5. Katz, L., and Donadio, S. (1993). Polyketide synthesis: prospects for hybrid antibiotics. Annu. Rev. Microbiol. *47*, 875–912.
6. Hutchinson, C.R., and Fujii, I. (1995). Polyketide synthase gene manipulation: a structure-function approach in engineering novel antibiotics. Annu. Rev. Microbiol. *49*, 201–238.
7. Pfeifer, B.A., and Khosla, C. (2001). Biosynthesis of polyketides in heterologous hosts. Microbiol. Mol. Biol. Rev. *65*, 106–118.
8. Gregory, M.A., Gaisser, S., Lill, R.E., Hong, H., Sheridan, R.M., Wilkinson, B., Petkovic, H., Weston, A.J., Carletti, I., Lee, H.L., et al. (2004). Isolation and characterization of pre-rapamycin, the first macrocyclic intermediate in the biosynthesis of the immunosuppressant rapamycin by *S. hygroscopicus*. Angew. Chem. Int. Ed. Engl. *43*, 2551–2553.
9. Wilcox, M.H., Hall, J., Pike, H., Templeton, P.A., Fawley, W.N., Parnell, P., and Verity, P. (2003). Use of perioperative mupirocin to prevent methicillin-resistant *Staphylococcus aureus* (MRSA) orthopaedic surgical site infections. J. Hosp. Infect. *54*, 196–201.
10. Fuller, A.T., Mellows, G., Woolford, M., Banks, G.T., Barrow, K.D., and Chain, E.B. (1971). Pseudomonic acid: an antibiotic produced by *Pseudomonas fluorescens*. Nature *234*, 416–417.
11. Chain, E.B., and Mellows, G. (1974). Structure of pseudomonic acid, an antibiotic from *Pseudomonas fluorescens*. J. Chem. Soc. Chem. Commun. 847–848.
12. Chain, E.B., and Mellows, G. (1977). Pseudomonic acid. Part 3. The structure of Pseudomonic acid B. J. Chem. Soc. Perkin Trans. I 318–322.
13. Feline, T.C., Jones, R.B., Mellows, G., and Phillips, L. (1977). Pseudomonic acid. Part 2. Biosynthesis of pseudomonic acid A. J. Chem. Soc. Perkin Trans. I 309–318.
14. Martin, F.M., AND Simpson, T.J. (1989). Biosynthetic studies on pseudomonic acid, a novel antibiotic of *Pseudomonas fluorescens*. J. Chem. Soc. Perkin Trans. I 207–209.
15. El-Sayed, A.K., Hothersall, J., Cooper, S.M., Stephens, E., Simpson, T.J., and Thomas, C.M. (2003). Characterization of the mupirocin biosynthesis gene cluster from *Pseudomonas fluorescens* NCIMB 10586. Chem. Biol. *10*, 419–430.
16. Shiozawa, H., Kagasaki, T., Kinoshita, T., Haruyama, H., Domon, H., Utsui, Y., Kodama, K., and Takahashi, S. (1993). Thiomarinol, a new hybrid antimicrobial antibiotic produced by a marine bacterium fermentation, isolation, structure, and antimicrobial activity. J. Antibiot. (Tokyo) *46*, 1834–1842.
17. Shiozawa, H., Shimada, A., and Takahashi, S. (1997). Thiomarinols D, E, F and G, new hybrid antimicrobial antibiotics produced by a marine bacterium; isolation, structure, and antimicrobial activity. J. Antibiot. (Tokyo) *50*, 449–452.
18. El-Sayed, A.K., Hothersall, J., and Thomas, C.M. (2001). Quorum-sensing-dependent regulation of biosynthesis of the polyketide antibiotic mupirocin in *Pseudomonas fluorescens* NCIMB 10586. Microbiol. *147*, 2127–2139.
19. Cooper, S.M., Cox, R.J., Crosby, J., Crump, M.P., Hothersall, J., Laosripaiboon, W., Simpson, T.J., and Thomas, C.M. (2005). Mupirocin W, a novel pseudomonic acid produced by targeted mutation of the mupirocin biosynthetic gene cluster. Chem. Commun. *2005*, 1179–1181.
20. Mendes, M.V., Recio, E., Fouces, R., Luiten, R., Martin, J.F., and Aparicio, J.F. (2001). Engineered biosynthesis of novel polyenes: a pimaricin derivative produced by targeted gene disruption in *Streptomyces natalensis*. Chem. Biol. *8*, 635–644.
21. Weber, J.M., Leung, J.O., Swanson, S.J., Idler, K.B., and McAlpine, J.B. (1991). An erythromycin derivative produced by targeted gene disruption in *Saccharopolyspora erythraea*. Science *252*, 114–117.
22. Mansuy, D. (1998). The great diversity of reactions catalyzed by cytochromes P450. Comp. Biochem. Physiol. C Pharmacol. Toxicol. Endocrinol. *121*, 5–14.
23. Urlacher, V.B., Lutz-Wahl, S., and Schmid, R.D. (2004). Microbial P450 enzymes in biotechnology. Appl. Microb. Biotechnol. *64*, 317–325.
24. Lowden, P.A.S., Bohm, G.A., Metcalfe, S., Staunton, J., and Leadlay, P.F. (2004). New rapamycin derivatives by precursor-directed biosynthesis. ChemBioChem *5*, 535–538.
25. Mantle, P.G., De Langen, M., and Teo, V.K. (2001). Differentiating the biosynthesis of pseudomonic acids A and B. J. Antibiot. (Tokyo) *54*, 166–174.
26. Sorensen, J.L., Auclair, K., Kennedy, J., Hutchinson, C.R., and Vederas, J.C. (2003). Transformations of cyclic nonaketides by *Aspergillus terreus* mutants blocked for lovastatin biosynthesis at the *lovA* and *lovC* genes. Org. Biomol. Chem. *1*, 50–59.
27. Whatling, C.A., Hodgson, J.E., Martin, K.R.B., Clarke, N.J., Franklin, C.H., and Thomas, C.M. (1995). Identification of a 60 kb region of the chromosome of *Pseudomonas fluorescens* NCIB 10586 required for the biosynthesis of pseudomonic acid. Microbiol. *141*, 973–982.
28. Hanahan, D. (1983). Studies on transformation of *Eschericia coli* with plasmids. J. Mol. Biol. *166*, 557–580.
29. Simon, R., Priefer, U., and Puhler, A. (1983). A broad host range mobilization system for in vivo genetic engineering: transposon mutagenesis in gram negative bacteria. Biotechnology (N. Y.) *1*, 784–791.
30. Kahn, M., Kolter, R., Thomas, C., Figurski, D., Meyer, R., Remaut, E., and Helinski, D.R. (1977). Plasmid cloning vehicles derived from plasmids ColE1, R6K and RK2. Methods Enzymol. *68*, 268–280.
31. Birnboim, H.C., and Doly, J. (1979). A rapid alkaline extraction procedure for screening recombinant palsmid DNA. Nucleic Acids Res. *7*, 1513–1523.
32. Sambrook, J., Fritsch, E.F., and Maniatis, T. (1989). Molecular Cloning: A Laboratory Manual (Cold Spring Harbor, NY: Cold Spring Harbor Laboratory Press).
33. Mullis, K., Faloona, F., Scharf, S., Saiki, R., Horn, G., and Erlich, H. (1986). Specific enzymatic amplification of DNA in vitro: the polymerase chain reaction. Cold Spring Harb. Symp. Quant. Biol. *51*, 263–273.
34. Sanger, F., Nicklen, S., and Coulson, A.R. (1977). DNA sequencing with chain-terminating inhibitors. Proc. Natl. Acad. Sci. USA *74*, 5463–5467.
35. Cohen, S.N., Chang, A.C.Y., and Hsu, H. (1972). Non-chromosomal antibiotic resistance in bacteria; genetic transformation of *Eschericia coli* by R factor DNA. Proc. Natl. Acad. Sci. USA *69*, 2110–2114.
36. Shiozawa, H., Kagasaki, T., Torikata, A., Tanaka, N., Fujimoto, K., Hata, T., Furukawa, Y., and Takahashi, S. (1995). Thiomarinol-B and thiomarinol-C, new antimicrobial antibiotics produced by a marine bacterium. J. Antibiot. (Tokyo) *48*, 907–909.